Lasers in Manufacturing Conference 2019

Buildup stability and height prediction for direct metal deposition

Daniel Eisenbarth[a*], Fabian Soffel[a], Konrad Wegener[b]

[a] *inspire AG, ETH Zürich, Technoparkstrasse 1, 8005 Zürich, Switzerland*
[b] *Institute of Machine Tools and Manufacturing, ETH Zürich, Leonhardstrasse 21, 8092 Zürich, Switzerland*

Abstract

Parts made by additive manufacturing consist of a multitude of layers that need to have a precise, controlled height. The process of direct metal deposition can lead to an unstable buildup behavior due to process deviations, which is often compensated by closed-loop control. This contribution analyses the process mechanisms and reveals that the powder catchment efficiency as a function of the standoff distance is mainly responsible for the inherent buildup stability. The influence of the powder nozzle and its suitability for multi-layer buildup is discussed based on a Gaussian distribution model of the powder stream. A recursive algorithm is developed that predicts the stability behavior and part height with the input of the measured powder distribution. Simulations and experiments show that a stable set of parameters exist in which certain process deviations are compensated inherently, whereas inappropriate process parameters lead to a distorted surface. It is concluded that closed-loop height control is not mandatory as long as the nozzle design and the process parameters are optimized for a stable direct metal deposition process.

Keywords: Additive manufacturing; Direct metal deposition; Buildup stability; Powder distribution; Powder nozzle design

1. Introduction

The additive manufacturing (AM) process of direct metal deposition (DMD) gains recently high attention in academia and industry. As the basic principle, a processing head creates a melt pool on a workpiece by a laser beam. By blowing metallic powder into the melt pool and moving the processing head, tracks, layers, and volumetric structures can be fabricated. The process originates from the established laser cladding technology, which is for instance used to apply wear-resistant coatings or to repair turbine blades as outlined by Kaierle et al., 2017. Such applications require only one or few layers. Since the shape and dimensions of the workpiece can be measured, the distance from the processing head to the workpiece can be kept constant. However, volumetric parts made by DMD consist of a multitude of stacked layers. To ensure an

* Corresponding author. Tel.: +41-446-337-956 .
E-mail address: eisenbarth@inspire.ethz.ch .

accurate part height with a flat top surface, the layer height needs to be controlled, either actively or passively. With the AM process of powder bed fusion, the layer height is set by lowering the build platform, which compensates height deviations inherently. With DMD, the volume of the actually deposited material determines the layer height. Small deviations of the deposited volume can propagate themselves layer by layer and lead to a deviating part height as shown by Zhu et al., 2012 and Tan et al., 2018. Ultimately, buildup instabilities can damage the processing head if the part grows unrestrained to the nozzle. Since the nominal distance from the nozzle tip to the workpiece, hereafter called standoff *S*, lies commonly in the range of a few millimeters, the risk of collision is present during DMD.

To improve the buildup stability, Sammons et al., 2019 developed a closed-loop control system that measures the height of each layer and adjusts either the height of the processing head or the powder flow rate for the next layer. Garmendia et al., 2019 apply a similar approach to a laser and wire AM system. Although closed-loop control systems show good results, the disadvantages of sensor integration such as increased costs, complexity, and processing time prevent their application. Furthermore, most industrial CNC machines do not allow an adaptation of the NC code during its execution, thus the tool path can only be modified by additional axes. One advantage of powder instead of wire deposition is that a self-stabilizing effect can be initiated that ensures a defined layer height and compensates certain deviations as further explained by Haley et al., 2019. In this contribution, the influence of the nozzle design and the generated powder stream onto layer stability is discussed. An algorithm is presented that predicts the buildup stability and part height for multi-layer DMD, based on measurements of the actual powder distribution. Experiments demonstrate the influence of the process parameters on the stability behavior.

2. Materials and methods

2.1. Modeling of the powder flow density

Most powder nozzles apply the principle of coaxial deposition, which means that the powder stream is coaxial to the laser beam and focuses in a certain standoff below the nozzle. Discrete coaxial deposition uses multiple discrete nozzles, whereas a continuous coaxial nozzle forms an annular gap. The left side of Figure 1 illustrates the DMD process with a continuous coaxial nozzle, creating a melt pool with a width w_m. Multiple overlapping tracks form a layer with a height Δh on a workpiece, which can be the substrate or the previous layer. The right side shows the nomenclature of the powder stream model. It is used for a first approximation of the powder flow density ρ_p and explains the influence of the nozzle design qualitatively. The origin of the coordinate system (x_n, z_n) lies at the center of the nozzle tip.

As further outlined by Eisenbarth et al., 2019, the powder flow density of a continuous coaxial nozzle can be modeled as superposition of two annular Gaussian distributions. As apparent from Figure 1, the cone of the powder stream has a radius μ as a function of the distance z from the nozzle tip. With a diameter d_a of the annular gap at the nozzle tip and a geometric focus S_a, the radius $\mu(z)$ is calculated as:

$$\mu(z) = d_a \frac{S_a - z}{S_a} \tag{1}$$

The stream is assumed to disperse gradually with a divergence angle φ_a below the nozzle. The inner and outer distribution widths $c_i(z)$ and $c_o(z)$ are calculated trigonometrically depending on the annular gap size t_a and on the cone angle γ_a:

$$c_{i/o}(z) = \frac{1}{\cos(\gamma_a \pm \varphi_a)} \left(\frac{t_a}{2} \cdot cos\varphi_a - z \cdot \frac{sin\varphi_a}{cos\gamma_a} \right) \tag{2}$$

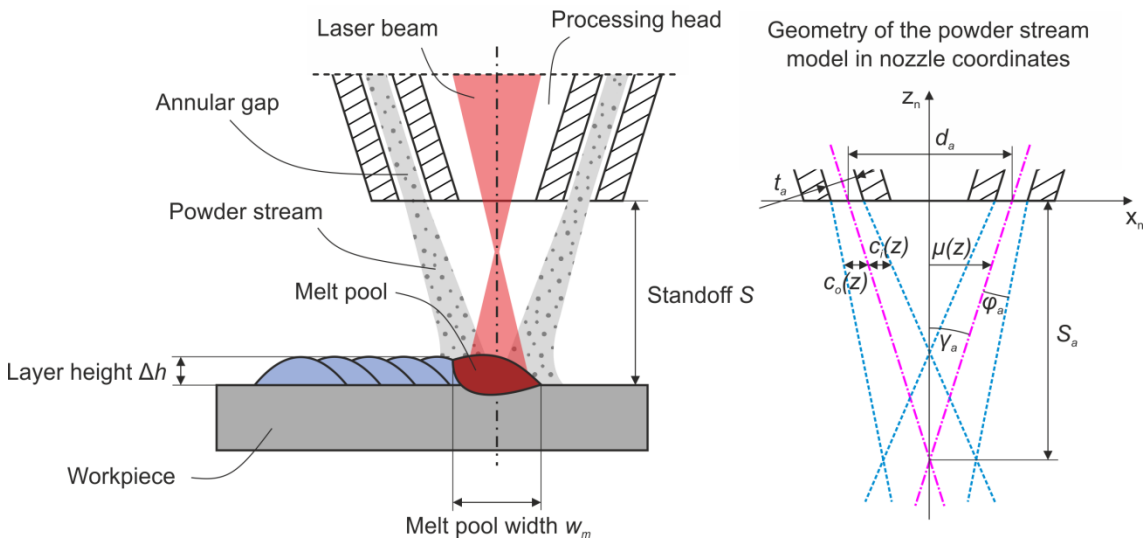

Fig. 1. Schematic DMD process, using a continuous coaxial nozzle and depositing one layer onto a workpiece (left). Geometry and designations of the powder stream model consisting of two annular Gaussian distributions (right)

Besides the radius μ as expected value and distribution width c, the Gaussian distribution requires a factor a for normalization in order that the integral of the powder flow density ρ_p equals 1 for an infinite surface, which corresponds to the total powder flow rate $\dot{m}_t$. Expressed in cylindrical coordinates with the unit 1/mm^2, ρ_p is a function of the radius r from the axis, polar angle θ, and vertical distance z:

$$\rho_p(r,\theta,z) = a\left[exp\left(-\frac{(r-\mu(z))^2}{c_{i/o}(z)^2}\right) + exp\left(-\frac{(r+\mu(z))^2}{c_{i/o}(z)^2}\right)\right] \quad (3)$$

The powder catchment efficiency η is defined as the percentage of powder that reaches the melt pool. In a simple approach that assumes a coaxial, circular melt pool, the modeled catchment efficiency is the surface integral of the powder flow density within the melt pool diameter in a certain standoff:

$$\eta(w_m,z) = \int_0^{2\pi}\int_0^{w_m/2} \rho_p(r,\theta,z) r\, dr\, d\theta \quad (4)$$

Figure 2 depicts the modeled powder stream of four exemplary nozzles. The pseudo-color images on the left show the stream distribution as stated in Equation (3) as a function of x and z. As the distribution is assumed to be rotationally symmetric, the polar angle is not considered. The geometric standoff lies in a constant distance of S_a = -10 mm. The annular gap diameter d_a changes from 4 mm (a) to 7 mm (b) and 10 mm (c and d). The modeled annular nozzle has a gap size t_a of 0.4 mm. Nozzles a), b), and c) show a realistic stream distribution width that grows with a divergence angle φ_a = 2.7°. Nozzle d) shows an ideal, non-dispersing stream with φ_a = 0°. On the right side of each pseudo-color plot, the catchment efficiency η as calculated from Equation (4) is plotted as a function of z for three melt pool diameters 1, 2, and 3 mm. The z-coordinate of maximum catchment efficiency, hereafter called powder focus S_f, is marked with a dashed line.

Plot d) shows that the powder focus S_f coincides with the geometric focus S_a of the theoretical powder cone for a perfect stream. However, for a more realistic, dispersing powder stream, the powder focus S_f

shifts upwards. This effect is significant for small cone angles γ_a as shown in plot a). Furthermore, a slim cone creates a plateau of high catchment efficiency, whereas the wide cones of plots b) and c) generate a pronounced peak that drops above and below the powder focus. The behavior of the catchment efficiency as a function of the standoff is critical for buildup stability as further explained in section 3.

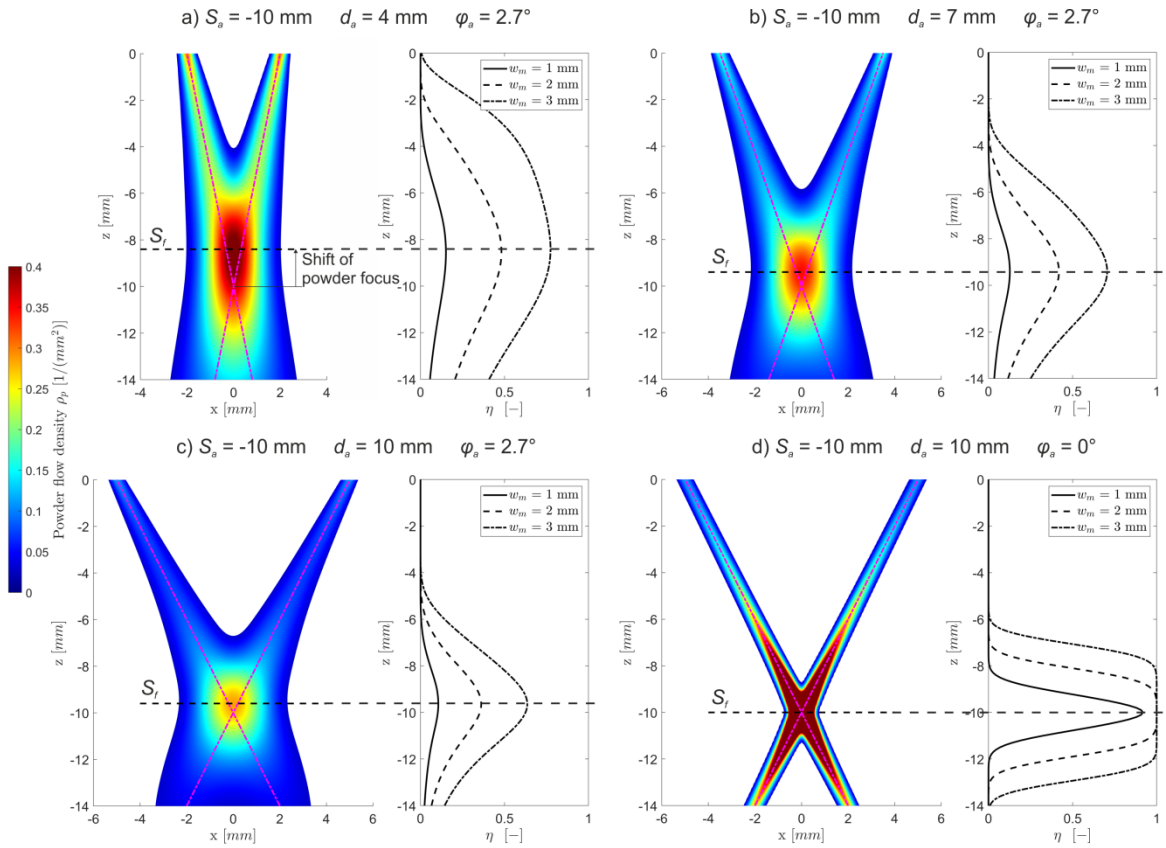

Fig. 2. Modeled powder distribution as a function of x and z for different annular gap diameters and divergence angles of the stream. On the right side of each pseudo-color image, the resulting catchment efficiency is plotted for melt pool widths of 1, 2, and 3 mm

2.2. Modeling of multi-layer buildup

A recursive algorithm was developed that calculates the part height in 2D as a function of x and z. Figure 3 introduces the different terms in the absolute buildup coordinate system (x_b, z_b). The function *h* denotes the part height at a specific lateral position *x'* and layer *i*. The height of the initial substrate is *h*(*x'*,*i*=0). The processing head fabricates a layer *i* in an absolute nozzle height *Z*(*i*) as constant for each layer, and with a local standoff *S*(*x'*,*i*) to the workpiece. It deposits a track that forms a layer with the incremental height *Δh*(x',*i*). The nozzle increment *ΔZ*(*i+1*) is the predefined distance that the nozzle moves up between layer *i* and *i*+1 .

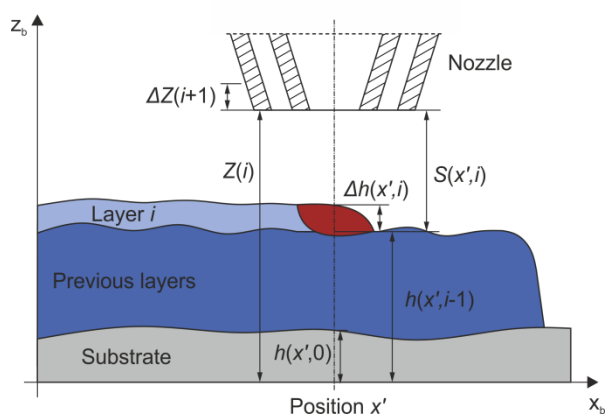

Fig. 3. Multi-layer model, designating the layer height *h* and nozzle height *Z* as a function of a specific lateral position *x'* and layer *i*

Neglecting edge effects and assuming a raster path with constant hatching distance *d*, the layer height can be deduced from the law of conservation of mass. Depositing a total powder flow rate $\dot{m}_t$ with a catchment efficiency η, the layer height Δh results as

$$\Delta h(x',i) = \frac{\dot{m}_t \cdot \eta(x',i)}{v_s \cdot d \cdot \rho} = K_{pr} \cdot \eta(x',i) \tag{5}$$

with a constant scan speed v_s and density ρ of the deposited and solidified material. Constant process parameters are substituted by the factor K_{pr}. Therefore, the layer height varies solely because of a varying catchment efficiency that depends on the local standoff and melt pool size:

$$\eta(x',i) = f\left(S(x',i), w_m\left(S(x',i)\right)\right) \tag{6}$$

The melt pool width can be measured from single tracks for the applied parameter set and different standoffs. In a first approximation, it is assumed that the melt pool size is only a function of the laser spot size, which in turn is a function of the standoff due to the laser beam caustic. This assumption is reasonable if the part is large enough to ensure a stationary DMD process, which means that the melt pool size is not influenced by varying heat flow conditions.

Since the melt pool is liquid, it levels out the waviness of the workpiece in the range of its diameter. Therefore, the influence of the surface waviness due to the overlapping spherical tracks on the part height is negligible, especially if the hatching direction is varied from layer to layer. The average part height h_{avg} at the current melt pool location *x'* is calculated in 2D as the surface integral of *h* divided by the melt pool width:

$$h_{avg}(x',i) = \frac{1}{w_m} \int_{x'-w_m/2}^{x'+w_m/2} h(x,i)\, dx \tag{7}$$

After finishing a layer *i*-1, the standoff for the fabrication of layer *i* at position *x'* is the current nozzle height minus the average part height of layer *i*-1:

$$S(x',i) = Z(x',i) - h_{avg}(x',i-1) \tag{8}$$

A calculation of the local catchment efficiency as a function of the standoff and the melt pool size requires either a database with measured values or a model according to section 2.1. Then, the total part height of layer *i* is a simple recursive function based on the previous average part height and on the local powder catchment efficiency multiplied with the constant process parameters as substituted by K_{pr}:

$$h(x',i) = h_{avg}(x',i-1) + \Delta h(x',i) = h_{avg}(x',i-1) + K_{pr} \cdot \eta(x',i) \quad (9)$$

2.3. Experimental setup

A prototype of a combined processing center for DMD and milling from the Swiss company Georg Fischer Machining Solutions was used for the experiments. The laser source emits light at a wavelength of 1070 nm with a maximum power of 1 kW. The continuous coaxial nozzle has a geometric standoff of 10 mm and an annular gap diameter of 5 mm. Rectangular blocks with a side length of 23 mm and composed of eight layers were fabricated from stainless steel powder type 1.4404 with a grain size distribution of 45 to 90 µm. All process parameters are listed in Table 1.

Table 1. DMD process parameters

Parameter [Unit]	Value
Laser power P_L [W]	900
Scan speed v_s [mm/min]	500
Hatching distance d [mm]	1.5
Nozzle increment ΔZ [mm]	1
Powder flow rate $\dot{m}_t$ [g/min]	6.7 to 9.1
Initial standoff S_{ini} [mm]	7 to 14
Melt pool width w_m at S = 10 mm [mm]	2.3

Four blocks were made with a varying powder flow rate and initial standoff to demonstrate the stability behavior. The tool path consists of a raster that changes its direction by 90° for each layer. The substrates are made from structural steel S235JRC. One layer was deposited prior to the blocks with a gap on the right and two additional tracks on the left, creating an indentation and a small hill which represent disturbances that can occur during DMD, for instance due to a worn workpiece surface or deviations of the process parameters from their nominal value. The initial standoff S_{ini} was measured from the undisturbed surface of the previously fabricated layer. Figure 4 depicts block number 3.

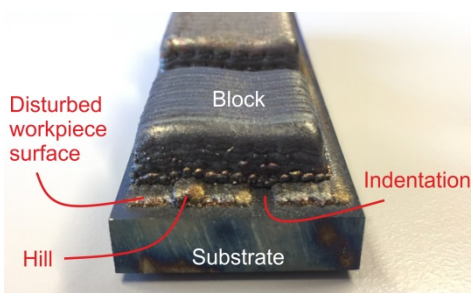

Fig. 4. Block number 3 made of eight layers. Processing started on a previously fabricated layer that contains artificial disturbances

3. Results and discussion

Measuring the powder flow density instead of using the simple Gaussian model enables a more precise prediction of the powder catchment efficiency. The 3D powder stream of the applied nozzle was measured by Eisenbarth et al., 2019 and is shown in Figure 5 on the left. The catchment efficiency according to Equation (4) was derived from these measurements as depicted on the right. The powder focus S_f is located 9 mm below the nozzle tip.

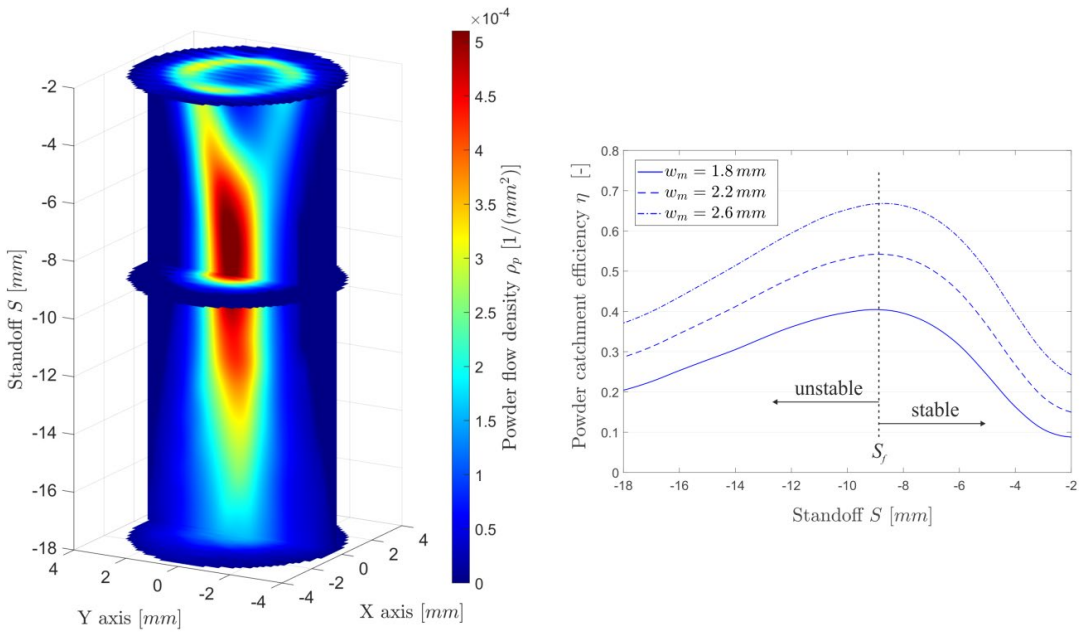

Fig. 5. Measured powder distribution in 3D with colors indicating ρ_p (left). Derived powder catchment efficiency as a function of the standoff for melt pool widths of 1.8, 2.2, and 2.6 mm (right, cited from Eisenbarth et al., 2019)

Buildup stability depends on the interaction between the predefined nozzle increment ΔZ and the actual layer height Δh, which determines the actual, local standoff. A negative feedback loop and therefore a stable buildup behavior is possible as soon as processing takes place closer to the nozzle than the powder focus distance: If the current layer is higher than the nozzle increment, the catchment efficiency decreases in the next layer, resulting in a smaller layer height and thus creating a counteracting effect. If the current layer height is smaller than the nozzle increment, it leads to a subsequent increase of catchment efficiency. The self-stabilizing effect is stronger for a steeper gradient of the catchment efficiency function. Thus, a distinctive powder focus as generated by a wide stream cone is more advantageous for stability than a flat plateau of high catchment efficiency created by a slim stream cone, as demonstrated by comparing nozzles a) and c) of Figure 2. If processing takes place at a greater standoff than the powder focus distance, the self-stabilizing effect inverts and creates a positive feedback loop: If the current layer height is smaller than the subsequent nozzle increment, the catchment efficiency drops further, and deviations propagate and amplify themselves from layer to layer.

With the recursive algorithm outlined in section 2.2 and the process parameters from Table 1, the buildup process of the four blocks was calculated in x and z as depicted on the left in Figure 6. The right side shows

the corresponding validation. The fabricated blocks were cut, polished, and etched to visualize the single layers. The raster paths have a parallel and perpendicular orientation to the image plane and alternate in each layer. The red lines indicate the shape of the intentionally deviated workpiece surface consisting of one layer with a gap and a hill that was fabricated prior to the blocks.

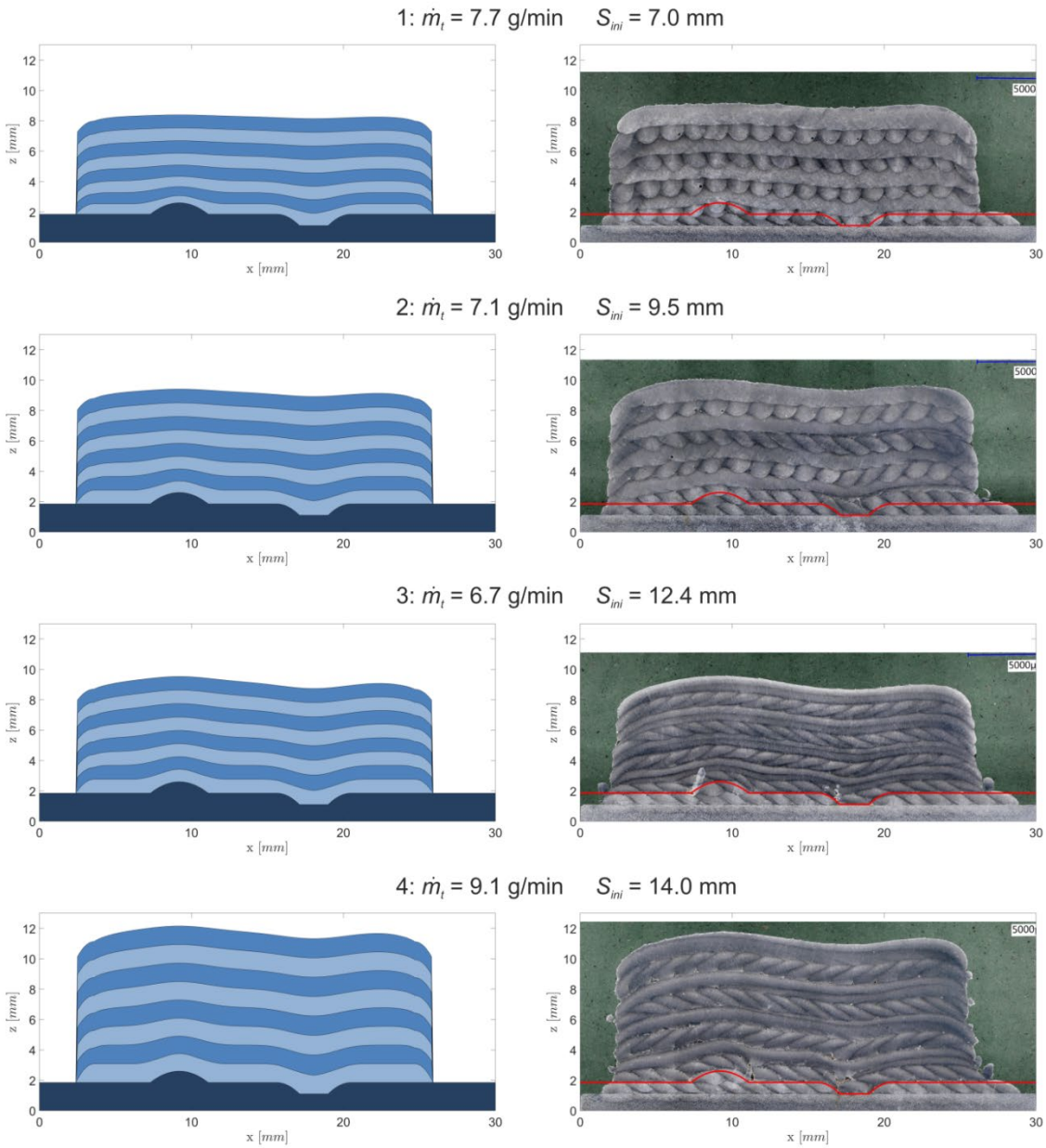

Fig. 6. Predicted part height (left) and cross-section of fabricated blocks (right) for four different parameters. The red lines indicate the shape of the initial surface with the artificial disturbances

The DMD process starts in an absolute height of 2 mm. When depositing eight layers with a nozzle increment of 1 mm, the optimal part height would be 10 mm. Since the goal of the experimental study is to provoke a stable and instable buildup behavior and to predict the part height for imperfect process conditions, both the powder flow rate and the initial standoff were varied randomly. All cross-sections show that the liquid melt pool levels out the waviness and the initial shape of the hill and indentation widens and blurs from layer to layer.

Block 1 was fabricated with a small initial standoff. Due to the strong balancing effect, the disturbances are reduced significantly after the first layers, and the final layer is almost flat. A small standoff is therefore advantageous for workpieces with high dimensional tolerances or if the DMD machine systems such as the motion axes or the powder feeder show deviations from their nominal performance. Repair applications can benefit, since a very stable DMD process does not require an individual tool path adaptation for each part. However, the process efficiency in terms of powder wastage is below its optimum. The initial standoff of Block 2 is similar to the powder focus of the nozzle, reaching the highest process efficiency there. The buildup behavior is characterized by an indifferent equilibrium, which means that the disturbances are propagated but not amplified. The melt pool blurs the hill and the indentation and creates an elongated wave in the final layer. Blocks 3 and 4 demonstrate the buildup instability caused by the high initial standoff. The first and second layers reveal that the disturbances tend to amplify themselves. Above, the melt pool levels out the peaks and the part shape transitions into the elongated wave.

Although the laser power and scan speed are constant for all experiments, the melt pool shape and dilution of blocks 1 and 2 differ significantly compared to blocks 3 and 4. Since processing is done with a defocused laser, the spot size increases and the maximum beam intensity decreases for larger standoffs. This leads to a deep and slim melt pool for small standoffs, and to a flat and wide melt pool for large standoffs.

4. Conclusion

When fabricating multi-layer structures with DMD, buildup stability plays an important role for the final part quality. The nozzle design determines the powder stream characteristics and the catchment efficiency as a function of the standoff and the melt pool size. A distinctive maximum of the powder catchment efficiency creates a strong self-stabilizing effect, if processing takes place closer to the nozzle than the distance to the focus of the powder. Such a powder distribution can be achieved by coaxial nozzles with a large cone angle. On the contrary, instability occurs if the actual standoff is greater than the powder focus distance. The destabilizing effect causes an amplification of disturbances from layer to layer, resulting in a wavy surface with low dimensional accuracy.

A recursive algorithm is proposed that predicts the layer height based on the catchment efficiency function. With a measured powder flow density of the applied nozzle and a known melt pool size for the specific process parameters, the accuracy of the prediction can be improved. The validation shows that both the predicted shape and total part height are in good agreement to cross-sections of the fabricated blocks. Deviations of the model can be caused by the melt pool, which is not circular in reality and may change its size from layer to layer due to varying heat flow conditions in the workpiece. However, the simple recursive algorithm shows that complex thermal simulations are not required to predict the buildup stability and layer height in a first approximation. Furthermore, the self-stabilizing effect makes closed-loop height control dispensable for DMD, if a suitable powder nozzle and optimized parameters are applied.

In the future, the algorithm shall be validated with different nozzle types, process parameters, and part geometries. Further challenges such as height prediction for five-axis processing and the fabrication of non-planar layers will be addressed.

Acknowledgements

The authors would like to acknowledge the contribution of the funding agency Innosuisse (grant number 25498) and of the companies GF Machining Solutions, GF Precicast, and ABB Turbo Systems Ltd.

References

Eisenbarth, D., Borges Esteves, P.M., Wirth, F., Wegener, K., 2019. Spatial powder flow measurement and efficiency prediction for laser direct metal deposition. in "*Surface and Coatings Technology*" 362, p. 397-408.

Garmendia, I., Pujana, J., Lamikiz, A., Flores, J., Madarieta, M., 2019. Development of an intra-layer adaptive toolpath generation control procedure in the laser metal wire deposition process. in "*Materials*" 12, no 3, p. 352.

Haley, J.C., Zheng, B., Bertoli, U.S., Dupuy, A.D., Schoenung, J.M., Lavernia, E.J., 2019. Working distance passive stability in laser directed energy deposition additive manufacturing. in "*Materials & Design*" 161, p. 86-94.

Kaierle, S., Overmeyer, L., Alfred, I., Rottwinkel, B., Hermsdorf, J., Wesling, V., Weidlich, N., 2017. Single-crystal turbine blade tip repair by laser cladding and remelting. in "*CIRP Journal of Manufacturing Science and Technology*" 19, p. 196-99.

Sammons, P.M., Gegel, M.L., Bristow, D.A., Landers, R.G., 2019. Repetitive process control of additive manufacturing with application to laser metal deposition. in "*IEEE Transactions on Control Systems Technology*" 27, no 2, p. 566-75.

Tan, H., Shang, W., Zhang, F., Clare, A.T., Lin, X., Chen, J., Huang, W., 2018. Process mechanisms based on powder flow spatial distribution in direct metal deposition. in "*Journal of Materials Processing Technology*" 254, p. 361-72.

Zhu, G., Li, D., Zhang, A., Pi, G., Tang, Y., 2012. The influence of laser and powder defocusing characteristics on the surface quality in laser direct metal deposition. in "*Optics & Laser Technology*" 44, no 2, p. 349-56.